



OPEN ACCESS

EDITED BY

Xiaojie Wang,
Chongqing University of Posts and
Telecommunications, China

REVIEWED BY

Cheng Fabin,
Huazhong University of Science and
Technology, China
Xiaomin Liu,
Chang'an University, China
Yating Liu,
Chongqing University of Posts and
Telecommunications, China

*CORRESPONDENCE

Juntao Pan
✉ 82021088@nxnu.edu.cn

RECEIVED 19 October 2025
REVISED 15 February 2026
ACCEPTED 19 February 2026
PUBLISHED 11 March 2026

CITATION

Wang S, Pan J, Shen X, Fan L and Ma X
(2026) Takagi-Sugeno fuzzy fault
estimator design for nonlinear dynamics
of autonomous ground vehicles.
Front. Comput. Sci. 8:1728300.
doi: 10.3389/fcomp.2026.1728300

COPYRIGHT

© 2026 Wang, Pan, Shen, Fan and Ma.
This is an open-access article distributed
under the terms of the [Creative
Commons Attribution License \(CC BY\)](#).
The use, distribution or reproduction in
other forums is permitted, provided the
original author(s) and the copyright
owner(s) are credited and that the
original publication in this journal is
cited, in accordance with accepted
academic practice. No use, distribution
or reproduction is permitted which does
not comply with these terms.

Takagi-Sugeno fuzzy fault estimator design for nonlinear dynamics of autonomous ground vehicles

Sujun Wang¹, Juntao Pan^{2*}, Xiuhong Shen³, Lu Fan¹ and Xiang Ma⁴

¹School of Physics and Electronic Information Engineering, Ningxia Normal University, Guyuan, China, ²School of Electrical and Information Engineering, Northern Minzu University, Yinchuan, China, ³School of Mathematics and Computer Science, Ningxia Normal University, Yinchuan, China, ⁴Hongta Tobacco (Group) Co., Ltd, Yuxi, China

In the context of cloud and edge computing for real-time fault diagnosis (FD) in autonomous ground vehicles (AGVs), this paper proposes a novel fault estimation method for AGV actuators. A two degrees-of-freedom nonlinear vehicle model is first used to characterize the AGV dynamics. Based on this model, a Takagi-Sugeno (TS) fuzzy observer is designed to estimate actuator fault signals. To handle unmeasurable premise variables, a nonlinear partitioning method reconstructs the TS fuzzy model into an N-TS fuzzy form. Unlike conventional TS fuzzy models with linear consequents, this reformulation incorporates the differential mean value theorem to explicitly address unmeasured nonlinearities—a common difficulty in TS fuzzy observer design. Using Lyapunov stability theory, the fault estimator is formulated as an optimization problem subject to strict linear matrix inequalities (LMIs), which can be solved efficiently with numerical tools. The proposed observer is validated through co-simulations in Simulink and CarSim, demonstrating its potential for deployment in cloud computing environments to enhance fault management in AGVs.

KEYWORDS

autonomous ground vehicles, fault estimation, nonlinear observer, Takagi-Sugeno fuzzy models, unmeasured premise variables

1 Introduction

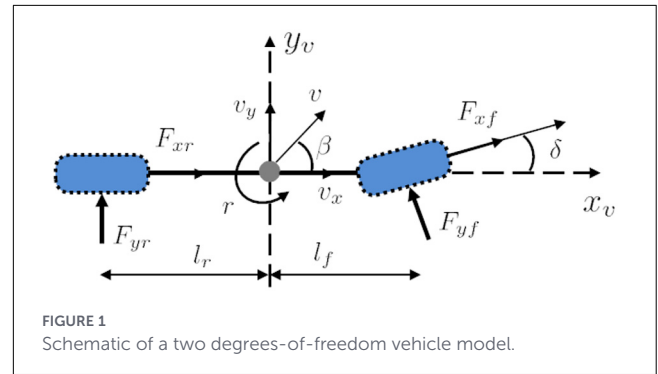
The advancement and deployment of cloud and edge computing technologies have significantly enhanced the active safety framework of AGVs (Zhou et al., 2022; Li et al., 2025b,a). A critical requirement for enabling these safety-critical functions is the reliable availability of real-time on-board sensor data (Deng et al., 2023; Zhang et al., 2025). However, the economic and technical constraints associated with sensor deployment often limit both the quantity and quality of such data, raising substantial concerns about its reliability and accuracy (Nguyen et al., 2018). These limitations underscore a crucial operational challenge: ensuring the fault-free operation of AGV systems—particularly the steering system—is vital for maintaining driving safety. Therefore, effective fault diagnosis and timely fault estimation are not merely technical objectives but operational necessities for AGV deployment (Mu et al., 2021; Nguyen et al., 2021a). In this context, while the existing literature offers various approaches for system monitoring and fault detection, a notable gap remains in accurately estimating fault signals under conditions of limited

measurability and system nonlinearity. This paper specifically addresses this challenge by developing a novel fault estimation methodology that overcomes the limitations of conventional approaches through an enhanced TS fuzzy framework capable of handling unmeasurable premise variables, thereby providing more robust and accurate fault diagnostics essential for the safe operation of AGVs.

Currently, accurate and timely fault estimation (FE) is critical for ensuring the operational safety of AGVs, serving as a fundamental input to fault-tolerant control systems that are essential to vehicle active safety (Zemzemi et al., 2019). While FE has drawn considerable research attention, existing methods often encounter practical limitations. For example, a fuzzy Proportional-Integral observer for TS fuzzy AGV systems was proposed in ElYoussefi and Oudghiri (2018), yet it is restricted to continuous-time models and involves a comparatively complex design procedure, limiting its applicability to real-world digital implementations. In response to these challenges, and inspired by Nguyen et al. (2021b) on handling unmeasured premise variables in observer design, this paper develops a discrete-time TS fuzzy observer to estimate actuator faults in AGV steering systems under disturbance conditions (Tanaka and Wang, 2004). The approach builds on the assumption that the second-order derivative of the fault signal is negligible, enabling system reformulation and facilitating a model-based estimator derived via direct Lyapunov stability analysis. The design is cast as a convex optimization problem in the form of LMIs, which can be efficiently solved with available numerical tools. By integrating the differential mean-value theorem (DMVT) into an N-TS fuzzy structure, the proposed estimator not only accommodates unmeasured nonlinearities but also delivers accurate fault estimates, thereby bridging the gap between theoretical design and real-time feasibility for AGV safety systems.

Building upon the foundation of TS fuzzy models for nonlinear vehicle dynamics, the primary limitation of existing methods lies in their reliance on measurable premise variables, which restricts their applicability to systems with partial state observability. To address this, we propose a reformulation of the AGV system into an N-TS fuzzy framework, which systematically integrates unmeasurable premise variables into a localized nonlinear consequent using the DMVT. This approach offers several distinct advantages over conventional TS fuzzy observers:

- (i) The proposed N-TS fuzzy framework provides notable advances over conventional TS approaches. Unlike existing methods that rely on fully measurable premise variables—restricting their use to systems with complete state observability—the N-TS formulation explicitly accommodates unmeasurable nonlinearities through a localized consequent structure. This enhances its applicability to AGV systems with partial or uncertain sensing. Moreover, by embedding finite-frequency characteristics of fault signals and disturbances—grounded in established physical insights—the observer design is optimized for realistic operational bandwidths (Liu et al., 2021; Wang et al., 2021), improving estimation accuracy while reducing tuning conservatism. These contributions collectively support a more adaptable and reliable fault estimation strategy for AGVs.



- (ii) The observer gains are derived through LMIs, ensuring both asymptotic stability of estimation errors and computational tractability for real-time implementation.
- (iii) The proposed fault estimation scheme is rigorously validated via co-simulations in Simulink and CarSim, demonstrating effective performance under varied driving scenarios, and showcasing its practical relevance for AGV safety-critical applications.

The structure of this paper is delineated as follows: Section 2 presents the derivation of a tailored N-TS fuzzy model for AGVs. It also outlines the preliminary preparations for the design of the fault estimation algorithm, including the observer and the differential mean value theorem. Useful Technicality such as lemma, theorem and LMI-based conditions are formulated in Section 3 for FE observer design. The visual representations of the simulation are detailed in Section 4, whereas Section 5 encompasses the concluding remarks.

2 Vehicle modeling

This section first describes the vehicle modeling utilized in observer-based fault estimation methodologies, then elaborates on the challenges in designing a fault estimation observer for AGV systems, and finally provides a collection of pertinent technical resources.

2.1 Nonlinear vehicle model

2.1.1 Vehicle dynamics model

This study adopts a 2-DOF nonlinear lateral vehicle model (Kang et al., 2023; Nguyen et al., 2024), which is depicted in Figure 1. Its dynamic model is given by:

$$\begin{aligned} \dot{v}_x &= \frac{T_{eng} - C_x v_x^2}{I_e} + v_y r \\ \dot{v}_y &= \frac{F_{yf} + F_{yr} - C_y v_y^2}{M_v} - v_x r \\ \dot{r} &= \frac{l_f F_{yf} - l_r F_{yr}}{I_z} + \frac{F_w}{I_z} \end{aligned} \quad (1)$$

TABLE 1 Vehicle nomenclature.

Symbol	Value	Description
M_v	1,481 [kg]	Automotive mass
I_e	443 [kgm ²]	Optimized retention of longitudinal momentum
I_z	1,807 [kgm ²]	Rotational inertia of a vehicle concerning the yaw axis
l_f	1.12 [m]	The measurement from the centroid to the anterior axle
l_r	1.5 [m]	The distance from the center of gravity to the rear axle
C_f	57,110 [N/rad]	Anterior lateral structural rigidity
C_r	58,100 [N/rad]	Lateral stiffness at the rear axle during vehicular cornering dynamics
C_x	0.37 [-]	Longitudinal aerodynamic resistance coefficient
C_y	0.42 [-]	Aerodynamic resistance lateral force coefficient

where v_x [m/s] denotes the longitudinal velocity, v_y [m/s] signifies the lateral velocity, r [rad/s] represents the yaw rate of the vehicle, and T_{eng} [Nm] indicates the torque input affecting the longitudinal dynamics (Deng et al., 2023; Zhang et al., 2025). The lateral wind force is expressed as F_w [N]. F_{yf} and F_{yr} correspond to the front tire forces and rear tire cornering forces, respectively, with other vehicle nomenclature provided in Table 1.

For our analysis, we assume typical driving conditions while adhering to the small angle approximation (Kang et al., 2025; Deng et al., 2023; Zhang et al., 2025). Furthermore, the lateral forces generated by the tires are directly related to the slip angles observed at each axle (Kang et al., 2025). Hence, the cornering forces at the front tires F_{yf} and at the rear tires F_{yr} can be approximated by:

$$F_{yf} = 2C_f \left(\delta - \frac{v_y + l_f r}{v_x} \right), F_{yr} = 2C_r \left(\frac{l_r r - v_y}{v_x} \right), \quad (2)$$

where δ is the front wheel steering angle. By analyzing Equations 1, 2, we can derive the governing nonlinear dynamics that characterize the behavior of the vehicle in the following manner:

$$\dot{x} = A_v(x)x + B_v u + D_v w. \quad (3)$$

In this scenario, the state vector of the vehicle is articulated as $x = [v_x \ v_y \ r]^T$, whereas the control input is represented by $u = [T_{eng} \ \delta]^T$. Additionally, the external disturbance is defined as $w = F_w$. The state-space matrices that pertain to the nonlinear vehicle model described in Equation 3 are delineated as follows:

$$A_v(x) = \begin{bmatrix} a_{11} & 0 & v_y \\ 0 & a_{22} & a_{23} \\ 0 & a_{32} & a_{33} \end{bmatrix}, B_v = \begin{bmatrix} b_{11} & 0 \\ 0 & b_{22} \\ 0 & b_{32} \end{bmatrix}, D_v = \begin{bmatrix} 0 \\ 0 \\ \frac{1}{I_z} \end{bmatrix},$$

with

$$\begin{aligned} a_{11} &= -\frac{C_x v_x}{I_e}, & b_{11} &= \frac{1}{I_e} \\ a_{22} &= -\frac{2(C_f + C_r)}{M_v v_x} - \frac{C_y v_y}{M_v}, & a_{23} &= \frac{2(C_r l_r - C_f l_f)}{M_v v_x} - v_x \\ a_{32} &= \frac{2(l_r C_r - C_f l_f)}{I_z v_x}, & a_{33} &= -\frac{2(C_f l_f^2 + C_r l_r^2)}{I_z v_x} \\ b_{22} &= \frac{2C_f}{M_v}, & b_{32} &= \frac{2l_f C_f}{I_z}. \end{aligned}$$

Furthermore, we acknowledge that although both the vehicle's longitudinal velocity v_x and the yaw rate r can be accurately measured, the lateral velocity v_y remains inaccessible due to financial limitations. As a result, the nonlinear model represented in Equation 3 can be restructured into the following descriptor form:

$$\begin{aligned} \dot{x} &= A_v(x)x + B_v u + D_v w, \\ y &= Cx, \end{aligned} \quad (4)$$

where

$$C = \begin{bmatrix} 1 & 0 & 0 \\ 0 & 0 & 1 \end{bmatrix}.$$

This research investigates the frequency and implications of actuator failures in AGVs. In pursuit of this objective, we analyze the failures associated with both the steering angle and Longitudinal torque, as detailed in Zhang and Wang (2017). The steering angle of the front-wheel steering, denoted as δ , together with the engine torque, represented by T , can be expressed mathematically in the following formulation:

$$\delta = \delta_d + b_\delta \delta_f, \quad T = T_d + b_T T_f. \quad (5)$$

In this framework, the parameters δ_d and T_d signify the desired steering angles for the front wheels as well as the associated engine torque, respectively. The variable δ_f represents the steering angle that is influenced by system faults, while T_f denotes the perturbation in engine torque. The coefficients b_δ and b_T are established based on the gain values of the actuators. We analyze model Equation 4 in conjunction with the fault model detailed in Equation 5, as follows:

$$\begin{aligned} \dot{x} &= A_v(x)x + B_v u_d + D_v w + F_v f, \\ y &= Cx, \end{aligned} \quad (6)$$

where

$$F_v = \begin{bmatrix} b_{11} b_T & 0 \\ 0 & b_{22} b_\delta \\ 0 & b_{32} b_\delta \end{bmatrix}, \quad u_d = \begin{bmatrix} T_d \\ \delta_d \end{bmatrix}, \quad f = \begin{bmatrix} T_f \\ \delta_f \end{bmatrix}.$$

2.1.2 Mathematical formulation of fault models

To rigorously characterize actuator faults, we consider two representative types:

(1) Bias injection fault: a constant or slowly varying bias is superimposed on the nominal control input:

$$u = u_d + f \cdot H(t - t_f), \quad (7)$$

where $\Delta u = [T_f, \delta_f]^T$ is the bias vector, $H(\cdot)$ is the Heaviside step function, and t_f denotes the fault onset time. In continuous time, the fault signal vector in Equation 6 becomes:

$$f = \begin{bmatrix} T_f \cdot H(t - t_f) \\ \delta_f \cdot H(t - t_f) \end{bmatrix}. \quad (8)$$

(2) Actuator scaling (loss-of-effectiveness) fault: The actuator's effectiveness degrades over time, modeled as a time-varying scaling factor:

$$f = \alpha(t) \odot u_d, \quad \alpha(t) \in [\alpha_{\min}, 1], \quad (9)$$

where \odot denotes element-wise multiplication. A linear degradation model is adopted:

$$\alpha(t) = 1 - \beta \cdot (t - t_f) \quad \text{for } t_f \leq t \leq t_f + \Delta t_{\text{fault}}, \quad (10)$$

with degradation rate $\beta > 0$. The corresponding fault signal is then:

$$f = (\alpha(t) - 1) \odot u_d. \quad (11)$$

These two explicit fault models cover common real-world actuator abnormalities and are used in the subsequent observer design and simulations.

Remark 1. In order to better represent the practical value of the designed observer, we considered the actual situation of the vehicle driving. We consider that the external disturbance during vehicle driving is mainly the obstructive effect of wind, and, this signal is a low frequency signal (Liu et al., 2021), we assume it is a constant and is $w = 800[\text{N}]$. In this work, in designing the fault estimator considering the faults of both steering angle and longitudinal torque, and considering the fault estimation performance when there is a disturbance signal in the actuator.

2.2 Fuzzy modeling for AGVs

In order to enable real-time execution, it is imperative to reconfigure the continuous model represented by Equation 6 into a discrete framework. For this transformation, we utilize the classical Euler method, defined by the equation $\dot{x}(t) \approx \frac{x_{k+1} - x_k}{s}$, where $s = 0.01$ signifies the sampling interval. As a result, the model Equation 6 is reformulated as follows:

$$\begin{aligned} x_{k+1} &= A(x_k)x_k + Bu_k + Dw_k + Ff_k, \\ y_k &= Cx_k, \end{aligned} \quad (12)$$

where

$$\begin{aligned} A(x_k) &= sA_v(x) + I, & B &= sB_v, \\ D &= sD_v, & F &= sF_v. \end{aligned}$$

and I is the identity matrix of suitable dimension, corresponding to $A(x_k)$.

In view of the fundamental physical constraints commonly present in typical driving scenarios (Nguyen et al., 2024), we can articulate a concise and comprehensive representation of the vehicle's state as follows:

$$S_x = \left\{ v_x \in [v_x, \bar{v}_x], v_y \in [v_y, \bar{v}_y], r \in [r, \bar{r}] \right\}. \quad (13)$$

Taking into account the parameters $v_x = 5$ [m/s], $\bar{v}_x = 30$ [m/s], $v_y = -1.5$ [m/s], $\bar{v}_y = 1.5$ [m/s], $r = -0.55$ [rad/s], and $\bar{r} = 0.55$ [rad/s], it is evident that the vehicle system described by Equation 12 exhibits three distinct nonlinear characteristics, which are referred to as premise variables: namely, $[\cdot]$, $\frac{1}{v_x}$, and v_y . Therefore, we define the vector of premise variables as $\varpi = \left[v_x \frac{1}{v_x} v_y \right]^T$. Utilizing the sector nonlinearity method as detailed in Tanaka and Wang (2004), one can systematically develop the standard eight-rule TS fuzzy model that accurately represents the nonlinear dynamics of the vehicle as articulated in:

$$\begin{aligned} x_{k+1} &= \sum_{i=1}^8 h_i(\varpi) A(x_k)x_k + Bu_k + Dw_k + Ff_k, \\ y_k &= Cx_k. \end{aligned} \quad (14)$$

The membership functions (MFs) represented as $h_i(\varpi)$, where i is an element of the index set \mathcal{I}_8 , are defined by the criteria $h_i(\varpi) \geq 0$ and the normalization condition $\sum_{i=1}^8 h_i(\varpi) = 1$. The local state-space matrices A_{v_i} , associated with each index $i \in \mathcal{I}_8$, are formulated by substituting the premise variables v_x , $\frac{1}{v_x}$, and v_y with their corresponding upper and lower bounds within the framework of $A(x_k)$. For conciseness, additional information regarding the local matrices and membership functions is deliberately omitted in this section. As of now, the conventional TS fuzzy representation has been widely utilized in the assessment of vehicle dynamics (Zhang et al., 2016). However, this traditional TS fuzzy framework introduces both theoretical and practical difficulties in the development of vehicle observers, primarily owing to the presence of unmeasured premise variables within the MFs Nguyen et al. (2021a). To overcome this notable limitation, we draw upon concepts from N-TS fuzzy modeling (Coutinho et al., 2020) and reformulate the vehicle system Equation 12 in the following manner:

$$\begin{aligned} x_{k+1} &= \sum_{i=1}^4 h_i(\xi) A_i x_k + Bu_k + Dw_k + Ff_k + g(\xi_k) + G\phi(x_k), \\ y_k &= Cx_k, \end{aligned} \quad (15)$$

where

$$A_i = \begin{bmatrix} 1 & sr & 0 \\ 0 & 1 - s \frac{2(C_f + C_r)}{M_v} V_x & 0 \\ 0 & s \frac{2(l_r C_r - C_f l_f)}{I_z} V_x & 1 \end{bmatrix}, \quad \xi = \begin{bmatrix} V_x \\ r \end{bmatrix},$$

$$g(\xi_k) = \begin{bmatrix} -s \frac{C_x v_x^2}{I_x} \\ s \frac{2(C_r l_r - C_f l_f)}{M_v v_x} r - v_x r \\ -s \frac{2(C_f l_f^2 + C_r l_r^2)}{I_z v_x} \end{bmatrix}, \quad G = \begin{bmatrix} 0 \\ -s \frac{C_y}{M_v} \\ 0 \end{bmatrix}.$$

and the system matrix A_i , for $i \in \mathcal{I}_4$, $\phi(x) = v_y^2$, $V_x = \frac{1}{v_x}$. The forthcoming section delineates the specifications pertaining to the local matrices alongside their associated moment functions, which are represented as $h_i(\xi)A_i$:

$$\begin{aligned} h_1(\xi)A_1 &= \frac{\bar{V}_x - V_x}{\bar{V}_x - \underline{V}_x} * \frac{\bar{r} - r}{\bar{r} - \underline{r}} * A(\underline{V}_x, r), \\ h_2(\xi)A_2 &= \frac{\bar{V}_x - V_x}{\bar{V}_x - \underline{V}_x} * \frac{v - \underline{r}}{\bar{r} - \underline{r}} * A(\underline{V}_x, \bar{r}), \\ h_3(\xi)A_3 &= \frac{V_x - \underline{V}_x}{\bar{V}_x - \underline{V}_x} * \frac{\bar{r} - r}{\bar{r} - \underline{r}} * A(\bar{V}_x, r), \\ h_4(\xi)A_4 &= \frac{V_x - \underline{V}_x}{\bar{V}_x - \underline{V}_x} * \frac{r - \underline{r}}{\bar{r} - \underline{r}} * A(\bar{V}_x, \bar{r}). \end{aligned}$$

the MFs, $\sum_{i=1}^4 h_i$ satisfy the following convex sum property:

$$0 \leq h_i(\xi) \leq 1, \quad \sum_{i=1}^4 h_i(\xi) = 1, \quad i \in \mathcal{I}_{n_r}. \quad (16)$$

Remark 2. The TS fuzzy models, which are derived from the sector nonlinearity approach, result in a polytypic embedding characterized by a vertex count of 2^n , where n represents the quantity of premise variables. As such, an increase in the number of premise variables leads not only to heightened computational requirements but also to an escalation in the structural complexity of the observational frameworks. Current methodologies for observer design in the context of AGVs rely on the Lipschitz condition that is intrinsic to conventional TS fuzzy modeling (Pan et al., 2020), culminating in a TS fuzzy model that is governed by eight fuzzy rules, as depicted in Equation 14. By reconfiguring the nonlinear descriptor system illustrated in Equation 14 into the format presented in Equation 15, it is feasible to attain a more accurate fuzzy representation that employs only four fuzzy rules. This reformulation serves to mitigate both the computational burden associated with observer design and the structural complexity of the observers necessary for real-time applications. Additionally, a salient feature of the N-TS fuzzy model delineated in Equation 15 is the evaluation of the nonlinear consequent $g(\xi_k)$ alongside the segregation of all measured premise variables within the unmeasured nonlinear consequent $\phi(x_k)$, thereby establishing a robust framework conducive to the design of fuzzy observers for AGVs.

2.3 Fault estimation problem formulation

Since the frequency of fault signals is limited in practical applications, using finite frequency technology for fault estimation can reduce its conservativeness (Zhang and Wang, 2017). We assume that the actuator fault signal f_k dynamics is represented as a triple integrator (Wang et al., 2022), namely,

$$\begin{bmatrix} f_{k+1} \\ f_{k+2} \\ f_{k+3} \end{bmatrix} = \begin{bmatrix} 0 & 1 & 0 \\ 0 & 0 & 1 \\ 1 & -3 & 3 \end{bmatrix} \begin{bmatrix} f_k \\ f_{k+1} \\ f_{k+2} \end{bmatrix}. \quad (17)$$

By analyzing Equations 14, (17), one can derive the following comprehensive N-TS fuzzy system,

$$\begin{aligned} \bar{x}_{k+1} &= \bar{A}(h)\bar{x}_k + T1(Bu_k + g(\xi_k)) + \bar{G}\phi(\bar{x}_k) + \bar{D}d_k \\ y_k &= \bar{C}\bar{x}_k, \end{aligned} \quad (18)$$

The system matrices in Equation 18 are give by:

$$\begin{aligned} \bar{A}(h) &= \begin{bmatrix} A(h) & F & 0 & 0 \\ 0 & 0 & 1 & 0 \\ 0 & 0 & 0 & 1 \\ 0 & 1 & -3 & 3 \end{bmatrix} & T1 &= \begin{bmatrix} I \\ 0 \\ 0 \\ 0 \end{bmatrix} & \bar{G} &= \begin{bmatrix} G \\ 0 \\ 0 \\ 0 \end{bmatrix} \\ \bar{D} &= [D^T \ 0 \ 0 \ 0]^T & \bar{C} &= [C \ 0 \ 0 \ 0], \end{aligned}$$

where $\bar{x}_k = [x_k^T \ f_k \ f_{k+1} \ f_{k+2}]^T$. and the MFs-dependent matrices are give by: $A(h) = \sum_{i=1}^{n_r} h_i(\xi)A_i$. It is important to acknowledge that the MFs adhere to the convex sum property as delineated in Equation 16.

For the purposes of estimating faults, we will examine the following configuration of the observer:

$$\begin{aligned} z_{k+1} &= N(h)z_k + L(h)y_k + MT1(g(\xi_k) + Bu_k) + MG\phi(\hat{x}_k), \\ \hat{x}_k &= z_k - Ey_k. \end{aligned} \quad (19)$$

In this context, z_k denotes the state variable observed by the observer, while \hat{x}_k represents the estimated value of \bar{x}_k . The matrices $N(h)$, $L(h)$, M , and E , which are contingent upon the membership functions, must be meticulously designed to fulfill specific criteria,

$$\begin{aligned} [N(h) \ L(h)] &= \sum_{i=1}^4 h_i(\xi_k) [N_i \ L_i], \\ M &= I + E\bar{C}. \end{aligned} \quad (20)$$

Considering the state estimation error defined as $e_k = x_k - \hat{x}_k$, one can deduce from Equations 19, 20 that

$$e_k = Mx_k - z_k. \quad (21)$$

Consequently, in light of the prevailing circumstances,

$$M\bar{A}(h) - N(h)M - L(h)\bar{C} = 0, \quad (22)$$

$$M\bar{D} = 0. \quad (23)$$

The dynamics of estimation error can be articulated based on the formulations presented in Equation 21 through Equation 23.

$$e_{k+1} = N(h)e_k + M\bar{G}\Delta\phi. \quad (24)$$

The presence of the mismatched term $\Delta\phi$ in Equation 24 presents a significant obstacle in the design of observers, as highlighted in Pan et al. (2020) and Pan et al. (2024). In order to adeptly address this term and ensure the convergence of the asymptotic estimation error, it is necessary to reformulate the expression for $\Delta\phi = \phi(\bar{x}_k) - \phi(\hat{x}_k)$ as a function of the estimation error e_k , as demonstrated in the subsequent Lemma 1.

2.4 Technical lemmas

Lemma 1. Zemouche et al. (2008) Let $g: \mathbb{R}^{n_x} \rightarrow \mathbb{R}^q$ be a differentiable function defined on the convex hull $\text{co}(a, b)$, where a and b are elements of \mathbb{R}^{n_x} . Under these conditions, it follows that there exist constant vectors c_i belonging to $\text{co}(a, b)$ such that c_i is neither equal to a nor to b for every index i within the index set \mathcal{I}_q .

$$g(a) - g(b) = \left(\sum_{i=1}^q \sum_{j=1}^{n_x} \sigma_q(i) \sigma_{n_x}^\top(j) \frac{\partial g_i}{\partial x_j}(c_i) \right) (a - b). \quad (25)$$

By utilizing Lemma 1 in relation to the function $\phi(\bar{x}_k)$, it can be deduced that there exist elements v_i belonging to the convex hull of the points x_k^e and \hat{x}_k^e , for indices i drawn from the set \mathcal{I}_1 ,

$$\begin{aligned} \Delta_\phi &= \left(\sum_{i=1}^1 \sum_{j=1}^9 \sigma_q(i) \sigma_{n_x}^\top(j) \frac{\partial \phi_i}{\partial x_j}(v_i) \right) (x_k - \hat{x}_k) \\ &= \underbrace{[\rho_{11} \ \rho_{12} \ \dots \ \rho_{19}]}_{\rho} e_k, \end{aligned} \quad (26)$$

where ρ_{ij} is defined as $\frac{\partial \phi_i}{\partial x_j}(v_i)$ for every pair $(i, j) \in \mathcal{I}_1 \times \mathcal{I}_9$. Given that x resides within the set S_x , as outlined in Equation 13, the parameter ρ is constrained to a bounded convex region denoted as S_ρ , characterized by its vertices, which are specified as follows:

$$V_\rho = \{\rho = [\rho_{11} \ \rho_{12} \ \dots \ \rho_{19}] : \rho_{ij} \in [\underline{\rho}_{ij}, \bar{\rho}_{ij}]\}.$$

Based on the formulations presented in Equations 24, 26, we can reformulate the dynamics of the residual as follows:

$$e_{k+1} = N(h, \rho) e_k, \quad (27)$$

where $N(h, \rho) = \sum_{i=1}^4 h_i(\xi_k) N_i(\rho_{ij})$ and

$$N_i(\rho_{ij}) = N_i + M\bar{G} \sum_{l=1}^1 \sum_{j=1}^9 \sigma_q(l) \sigma_{n_x}^\top(j) \rho_{lj}. \quad (28)$$

The formulation of the observer design problem can be articulated as follows.

Problem 1. In the context of nonlinear vehicle dynamics represented in N-TS form, achieving an effective estimation of faults for AGVs necessitates that the state estimate \hat{x}_k , the fault signal f_k , and its corresponding estimation \hat{f}_k converge asymptotically. Additionally, it is crucial to ascertain the matrices $N(h)$, $L(h)$, M , and E associated with the observer described in Equation 19. By employing arguments grounded in Lyapunov's theory, this study delineates a feasible and systematic approach to address the aforementioned observer design challenge.

3 Fault estimation observer design for vehicle system

In this section, we shall initially revisit the following lemma and theorem, which will serve as foundational components in the formulation of the principal outcomes presented in this manuscript.

3.1 Useful technicality

The subsequent lemma plays a pivotal role in facilitating the convexification process associated with the design of observers.

Lemma 2. Rao and Mitra (1971) Let us examine the matrix $W \in \mathbb{R}^{m \times n}$ where $m \geq n$ and the matrix $Z \in \mathbb{R}^{k \times n}$. The matrix X , defined as $X = ZW^\dagger + Y(I - WW^\dagger)$, where Y is an arbitrary matrix in $\mathbb{R}^{k \times n}$, serves as a solution to the equation $XW = Z$ under the prerequisite that the relation $ZW^\dagger W = Z$ is satisfied.

The subsequent theorem establishes the foundational theoretical framework necessary for the realization of our objective in designing a fault estimation observer.

Theorem 1. Examine the observer configuration described in Equation 19 under the stipulations outlined in Equations 20, 22. The stability of the estimation error dynamics characterized by Equation 27 is ensured if there exist positive definite matrices $P(h) > 0$, $N(h)$ that are dependent on membership functions, alongside matrices R , M , and E , satisfying the requisite conditions,

$$\begin{bmatrix} P(h) & * \\ RN(h, \rho) R + R^\top - P(h_+) \end{bmatrix} > 0, \quad (29)$$

for $h, h_+ \in \Omega$, $\rho \in S_\rho$, and in block matrices, the notation \star represents the components inferred from symmetry.

proof 1. To analyze the error system represented by Equation 27, we perform pre- and post-multiplication of Equation 29 by the matrix $[I \ -N(h, \rho)]^\top$ and its conjugate transpose. This operation yields a derived expression that facilitates further examination of the underlying dynamics.

$$N(h, \rho)^\top P(h_+) N(h, \rho) - P(h) < 0. \quad (30)$$

In the context of analyzing asymptotic stability, we employ a candidate fuzzy Lyapunov function as a primary tool for our investigation,

$$V(e_k) = e_k^\top P(h) e_k, \quad (31)$$

with $P(h) > 0$. The variation of the fuzzy Lyapunov function Equation 31 along the trajectory of system Equation 27 is defined as follows:

$$\begin{aligned} \Delta V &= V(e_{k+1}) - V(e_k) \\ &= e_k^\top \left(N(h, \rho)^\top P(h_+) N(h, \rho) - P(h) \right) e_k. \end{aligned} \quad (32)$$

From Equations 30, 32, it can be deduced that the variation in the Lyapunov function, denoted as ΔV , is less than zero for all instances where $e_k \neq 0$. This observation effectively completes the proof.

3.2 LMI-based fault estimation observer design

The subsequent theorem presents a numerically feasible solution for the design of the finite element observer as articulated in Problem 1.

Theorem 2. Examine the observer framework delineated in Equation 19 under the stipulations set forth in Equations 20, 22. The stability of the estimation error system characterized by Equation 27 is guaranteed if there exist matrix functions dependent on h , specifically $P(h) > 0$ and $N(h)$, along with matrices R , M , and E , such that the required conditions are met,

$$\begin{bmatrix} P(h) \\ \Psi \mathcal{A}(h, p) - X_i \bar{C} R + R^T - P(h_+) \end{bmatrix} > 0, \quad (33)$$

for $h, h_+ \in \Omega$, $\rho \in S_\phi$, and

$$\mathcal{A}(h, p) = \bar{A}_i + \bar{G} \sum_{l=1}^1 \sum_{j=1}^5 \sigma_1(l) \sigma_5^T(j) \rho_{lj}, \quad (34)$$

$$\Psi = R + (RU + ZV)\bar{C}. \quad (35)$$

proof 2. From Equations 20, 42, we can obtain

$$E(\bar{C}\bar{D}) = -\bar{D}. \quad (36)$$

Due to the complexities associated with the nonlinear matrix equality presented in equation (18) and the corresponding nonlinear matrix inequality outlined in equation (20), along with their inherent dependency on the matrix function (MF), it is not feasible to directly apply Theorem 2 for the design of the finite-time (FE) observer. In light of this observation, we propose leveraging Lemma 2, with the following assumptions: matrix \bar{C} possesses full row rank, matrix \bar{D} exhibits full column rank, and the rank of product $\bar{C}\bar{D}$ is equivalent to the rank of \bar{D} , we can derive the necessary results.

$$E = -\bar{D}(\bar{C}\bar{D})^\dagger + Y(I - (\bar{C}\bar{D})(\bar{C}\bar{D})^\dagger). \quad (37)$$

To facilitate the calculation, we can define,

$$U = -\bar{D}(\bar{C}\bar{D})^\dagger, \quad (38)$$

$$V = I - (\bar{C}\bar{D})(\bar{C}\bar{D})^\dagger, \quad (39)$$

$$X_i = RH_i, \quad (40)$$

$$Z = RY. \quad (41)$$

From Equations 37, 41, we can obtain Equation 29 Note let us define,

$$H_i = L_i + N_i F. \quad (42)$$

Consequently, upon analyzing Equations 22, 23, 42, one can deduce that

$$N_i = M\bar{A}_i - H_i \bar{C}. \quad (43)$$

From Equations 42, 43, we can obtain

$$L_i = H_i(I + \bar{C}E) - M\bar{A}_i E. \quad (44)$$

The algorithm for the fault estimation observer design of autonomous vehicles is summarized in Figure 2.

This concludes the proof.

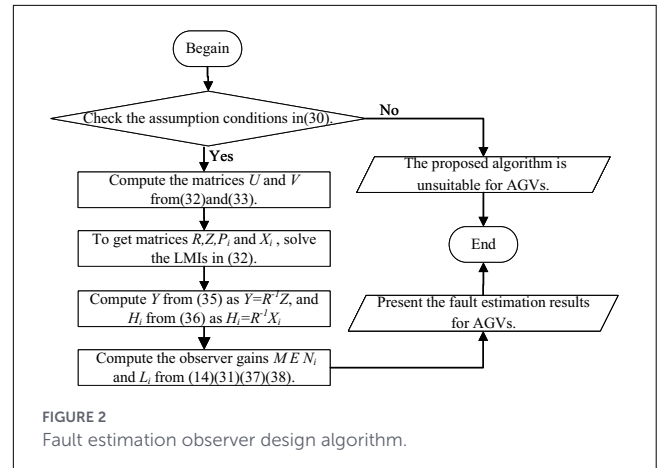


FIGURE 2 Fault estimation observer design algorithm.

4 Experiments and analysis

This section presents illustrative results to validate the efficacy of the proposed TS fuzzy fault estimation observer in simultaneously estimating AGV dynamics and actuator fault signals. The simulations are conducted in a co-simulation framework integrating MATLAB/Simulink and CarSim. A high-fidelity AGV model is developed in CarSim, with key parameters summarized in Table 1, including a rear drive-toque ratio of [4:1], maximum power of 150[kW], and operation on dry asphalt road with a friction coefficient $\mu = 1.0$. The proposed observer is implemented in Simulink, and its parameters are obtained by solving the LMIs in Theorem 2 using the SDPT3 solver. Its pseudocode is presented in Algorithm 1.

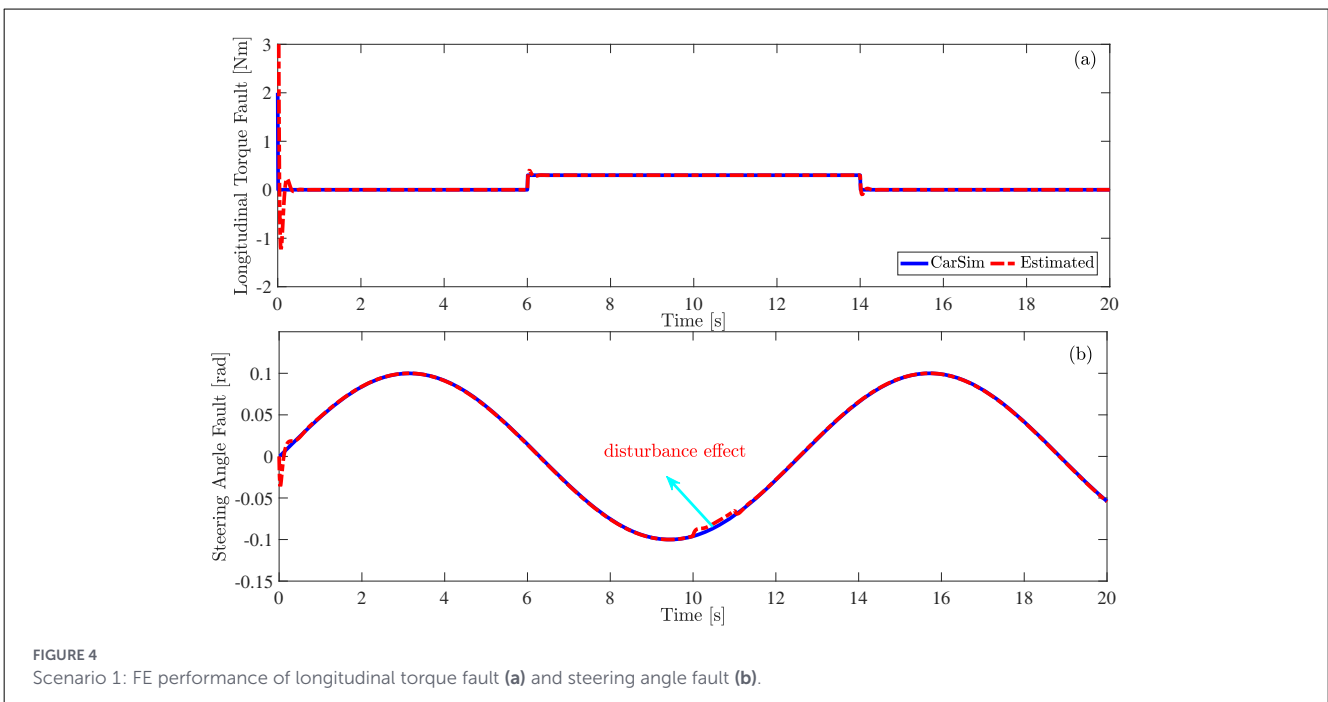
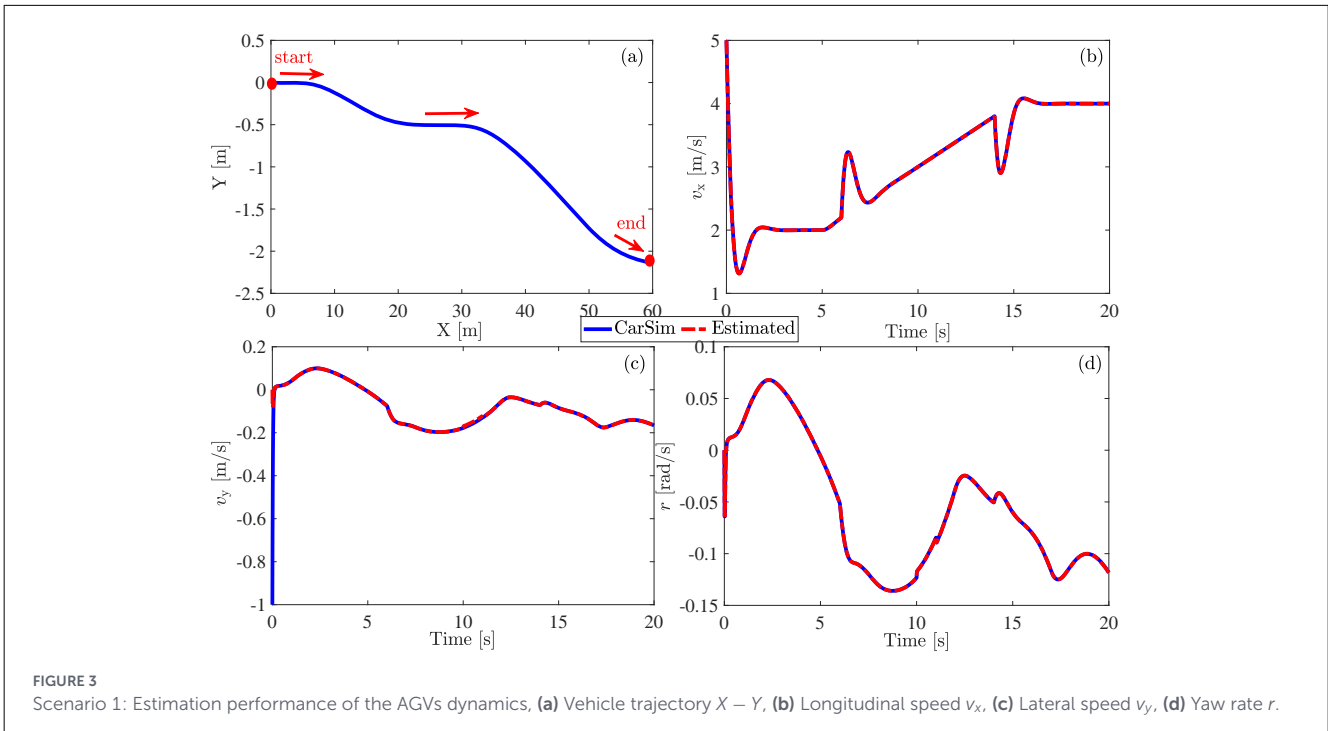
Require: System matrices A_i, B, C, D, F, G ; bounds on v_x, v_y, r ; sampling time s ; disturbance w .

Ensure: Observer gains N_i, L_i, M, E ; estimated states \hat{x}_k ; fault estimates \hat{f}_k .

- 1: Construct the N-TS fuzzy model 15 using sector nonlinearity and DMVT.
- 2: Formulate the augmented system 18 with fault dynamics 17.
- 3: Define observer structure as in 19.
- 4: Solve LMIs in Theorem 2 using SDPT3 solver to obtain R, Z, P_i and X_i , for $i \in \mathcal{I}_4$.
- 5: Compute N_i and L_i from Equations 23 and 44.
- 6: **for** each time step k **do**
- 7: Measure y_k .
- 8: Compute $\hat{x}_k = z_k - E y_k$.
- 9: Update observer state:

$$z_{k+1} = N(h)z_k + L(h)y_k + MT_1(g(\xi_k) + Bu_k) + MG\phi(\hat{x}_k).$$
- 10: Extract fault estimate \hat{f}_k from \hat{x}_k .
- 11: **end for**

Algorithm 1. Fault estimation observer design.



Two distinct experimental scenarios with different actuator fault types are designed to evaluate observer performance. The simulation results from CarSim are shown in Figures 3–6. Figures 3, 5 illustrate the vehicle’s trajectory and dynamic states, while Figures 4, 6 present the fault estimation performance for longitudinal torque and steering angle faults, respectively. These results collectively demonstrate the observer’s capability to accurately reconstruct both system states and fault signals under realistic driving conditions.

4.1 Scenario 1: driving with a random leftward vehicle trajectory

In this test scenario, the 2-DOF vehicle executes a sequence of maneuvers, specifically proceeding straight, making a right turn, and then continuing straight before executing another right turn, as illustrated in Figure 3a. The initial conditions of the observer are set to $[5, -1, 0]$. The AGV system experiences a sudden fault signal characterized by

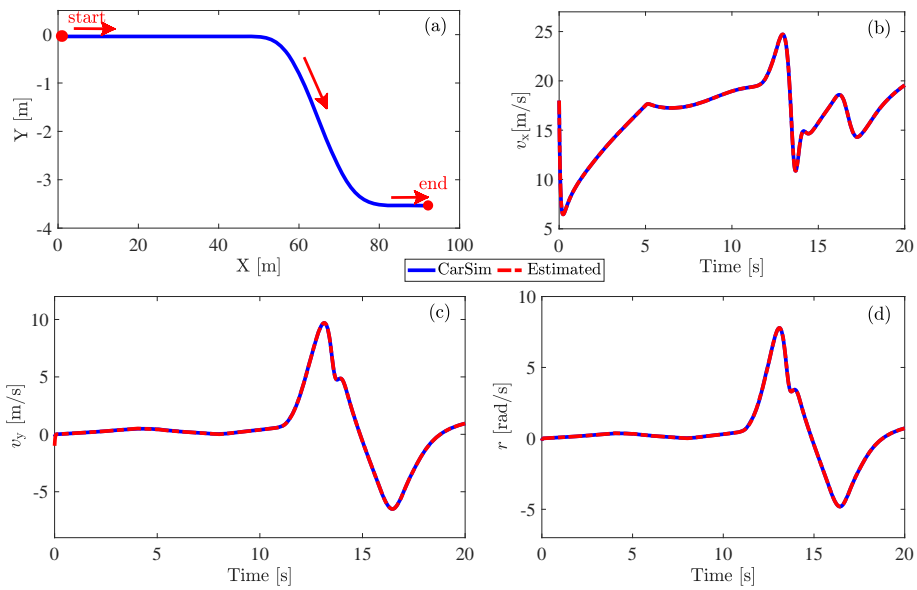


FIGURE 5 Scenario 2: Estimation performance of the AGVs dynamics, (a) vehicle trajectory $X - Y$, (b) longitudinal speed v_x , (c) lateral speed v_y , (d) yaw rate r .

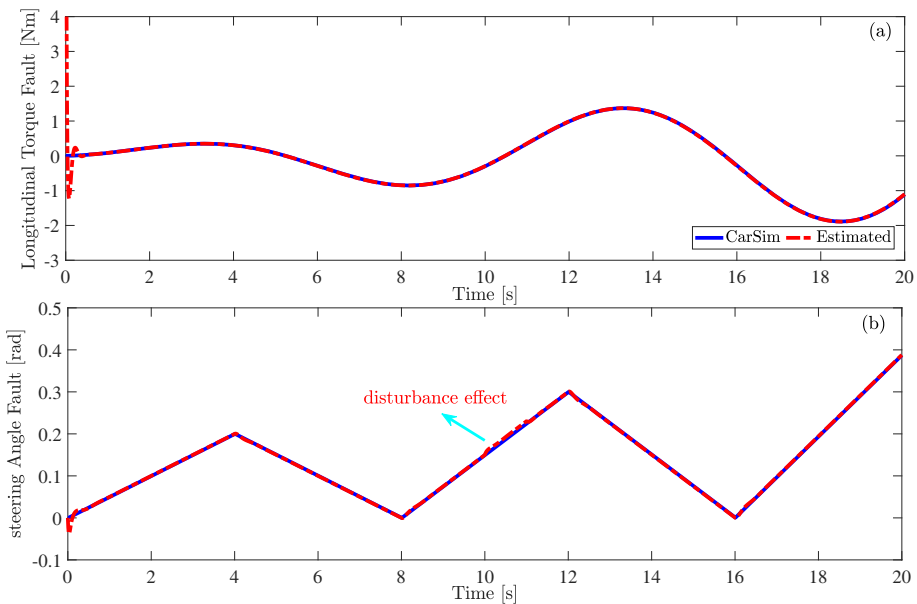


FIGURE 6 Scenario 2: FE performance of longitudinal torque fault (a) and steering angle fault (b).

an amplitude of 0.3[Nm] affecting the longitudinal torque, alongside a repetitive fault signal with an amplitude of 0.1[rad] and a frequency of 0.5[rad/s] impacting the steering angle, As shown by the blue line in Figure 4. As shown in Figure 3c, the estimated unmeasurable premise variables v_y of the AGV rapidly align with their corresponding measurements through the designed fuzzy fault estimation observer, even in the presence of lateral wind disturbances occurring between 10 and 11 s. Furthermore, Figure 4 demonstrates that both the longitudinal torque fault and the steering angle fault can be

accurately estimated using the proposed fuzzy fault estimation observer methodology.

4.2 Scenario 2: driving with random lane-changing

In this context, the amplitude of the fault signal is progressively amplified to replicate the actual variation observed

in vehicle fault signals. This approach aims to further assess the estimation capabilities of the proposed fault estimation observer without necessitating any information pertaining to the actuator faults in the vehicle's steering system. Accordingly, as depicted in Figure 5a, the vehicle performs a lane change maneuver between 13 and 21 seconds. The initial longitudinal velocity of the vehicle, represented as v_x , is 5[m/s]; the initial lateral velocity, denoted as v_y , is -1[m/s]; and the yaw rate, indicated as r , is 0[rad/s]. Fault signals are represented by blue lines in Figure 6. In alignment with the preceding two test scenarios, Figures 5c, 6 distinctly illustrate that the proposed methodology can not only effectively estimate the dynamic characteristics of AGVs but also accurately quantify the fault signal.

4.3 Scalability discussion

The simulation scenarios in Sections 4.1–4.2 represent worst-case conditions: fault intensity is set to the maximum design limit of 10% of nominal input, faults persist throughout the entire 20 s simulation, and both actuators are simultaneously compromised. As demonstrated in Figures 3–6, the proposed observer maintains reliable estimation under these extreme conditions, confirming its scalability to the most demanding fault scenarios in real-world AGV applications.

5 Conclusions

This study focuses on the steering angle control system of AGVs and develops a dynamic model for the AGV system. To address the issue of unmeasured premise variables in the TS fuzzy model, a nonlinear partitioning approach is employed to restructure the TS fuzzy model specific to the AGV dynamics. This restructuring results in an enhanced TS fuzzy model that incorporates localized nonlinear sub-models, termed the N-TS fuzzy model. Furthermore, the differential mean value theorem is utilized to manage the nonlinear components effectively. To mitigate the design's conservatism, fault estimation algorithms are devised using fault signals associated with lateral torque and steering angle, confined to finite frequency domains. The efficacy of these fault estimation algorithms is assessed in relation to the impact of these actuator fault signals on the AGV system. Leveraging Lyapunov stability theory, the LMI conditions for the fault estimation algorithms are formulated and resolved through numerical solvers. Ultimately, co-simulations conducted in MATLAB/Simulink and CarSim demonstrate that the proposed fault estimation algorithms achieve superior performance in fault estimation, particularly when integrated with cloud computing and edge computing frameworks for real-time monitoring and decision-making.

Data availability statement

The raw data supporting the conclusions of this article will be made available by the authors, without undue reservation.

Author contributions

SW: Writing – original draft. JP: Writing – review & editing. XS: Writing – review & editing. LF: Writing – review & editing. XM: Data curation, Validation, Investigation, Writing – review & editing.

Funding

The author(s) declared that financial support was received for this work and/or its publication. This work was supported in part by the university-level research project of Ningxia Normal University under Grant NSDXJQN07, in part by the Ningxia Natural Science Foundation of China under Grant 2024AAC03323, in part by the Ningxia Normal University Intelligent Perception Engineering Technology Research Center.

Conflict of interest

XM was employed by Hongta Tobacco (Group) Co., Ltd.

The remaining author(s) declared that this work was conducted in the absence of any commercial or financial relationships that could be construed as a potential conflict of interest.

Generative AI statement

The author(s) declared that generative AI was not used in the creation of this manuscript.

Any alternative text (alt text) provided alongside figures in this article has been generated by Frontiers with the support of artificial intelligence and reasonable efforts have been made to ensure accuracy, including review by the authors wherever possible. If you identify any issues, please contact us.

Publisher's note

All claims expressed in this article are solely those of the authors and do not necessarily represent those of their affiliated organizations, or those of the publisher, the editors and the reviewers. Any product that may be evaluated in this article, or claim that may be made by its manufacturer, is not guaranteed or endorsed by the publisher.

References

- Coutinho, P., Araújo, R., Nguyen, A.-T., and Palhares, R. (2020). A multiple-parameterization approach for local stabilization of constrained Takagi-Sugeno fuzzy systems with nonlinear consequents. *Inf. Sci.* 506, 295–307. doi: 10.1016/j.ins.2019.08.008
- Deng, H., Zhao, Y., Nguyen, A.-T., and Huang, C. (2023). Fault-tolerant predictive control with deep-reinforcement-learning-based torque distribution for four in-wheel motor drive electric vehicles. *IEEE/ASME Trans. Mechatron.* 28, 668–680. doi: 10.1109/TMECH.2022.3233705
- El Youssef, N. and Oudghiri, M. (2018). “Fault estimation and tolerant control for vehicle lateral dynamics,” in *2018 7th International Conference on Systems and Control (ICSC)*, 213–218.
- Kang, Z., Li, T., and Fan, X. (2023). Delay-dependent anti-disturbance control of electric vehicle based on collective observers. *AIMS Mathemat.* 8, 14684–14703. doi: 10.3934/math.2023751
- Kang, Z., Li, T., and Fan, X. (2025). Dual-observer based resilient control for vehicle trajectory tracking under tri-modal cyber attacks. *IET Control Theory Appl.* 19:e70072. doi: 10.1049/cth2.70072
- Li, C., Tan, C., Liu, G., Wen, Y., Wang, Y., and Li, K. (2025a). DC-ORAM: an oram scheme based on dynamic compression of data blocks and position map. *IEEE Trans. Comp.* 74, 1495–1509. doi: 10.1109/TC.2025.3533089
- Li, C., Yuntao, S., Zhou, Z., Zhao, Z., Wen, Y., Chen, J., and Wei, J. (2025b). Multi-agent reinforcement learning-based cost-efficient edge server deployment in CPSS. *IEEE Trans. Comput. Soc. Syst.* 172, 1–13. doi: 10.1109/TCSS.2025.3616223
- Liu, C.-Z., Li, L., Yong, J.-W., Muhammad, F., and Cheng, S. (2021). An innovative finite frequency h_∞ . *IEEE Trans. Intellig. Transport. Syst.* 22, 1553–1561. doi: 10.1109/TITS.2020.2971972
- Mu, Y., Zhang, H., Xi, R., and Gao, Z. (2021). State and fault estimations for discrete-time T-S fuzzy systems with sensor and actuator faults. *IEEE Trans. Circuits Syst. II: Express Briefs.* 68, 3326–3330. doi: 10.1109/TCSII.2021.3067708
- Nguyen, A.-T., Dinh, T.-Q., Guerra, T.-M., and Pan, J. (2021a). Takagi-sugeno fuzzy unknown input observers to estimate nonlinear dynamics of autonomous ground vehicles: theory and real-time verification. *IEEE/ASME Trans. Mechatron.* 26:1. doi: 10.1109/TMECH.2020.3049070
- Nguyen, A.-T., Frezzatto, L., Guerra, T.-M., and Delprat, S. (2024). Cost-effective estimation of vehicle lateral tire-road forces and sideslip angle via nonlinear sampled-data observers: theory and experiments. *IEEE/ASME Trans. Mechatron.* 29, 4606–4617. doi: 10.1109/TMECH.2024.3382777
- Nguyen, A.-T., Pan, J., Guerra, T.-M., and Wang, Z. (2021b). Avoiding unmeasured premise variables in designing unknown input observers for takagi-sugeno fuzzy systems. *IEEE Cont. Syst. Lett.* 5, 79–84. doi: 10.1109/LCSYS.2020.2999028
- Nguyen, A.-T., Sentouh, C., and Popieul, J.-C. (2018). Sensor reduction for driver-automation shared steering control via an adaptive authority allocation strategy. *IEEE/ASME Trans. Mechatron.* 23, 5–16. doi: 10.1109/TMECH.2017.2698216
- Pan, J., Nguyen, A.-T., Guerra, T.-M., and Ichalal, D. (2020). A unified framework for asymptotic observer design of fuzzy systems with unmeasurable premise variables. *IEEE Trans. Fuzzy Syst.* 29:1. doi: 10.1109/TFUZZ.2020.3009737
- Pan, J., Nguyen, A.-T., Wang, S., Deng, H., and Zhang, H. (2024). Fuzzy unknown input observer for estimating sensor and actuator cyber-attacks in intelligent connected vehicles. *Automot. Innovat.* 6, 164–175. doi: 10.1007/s42154-023-00228-1
- Rao, C. R. and Mitra, S. K. (1971). *Generalized Inverse of Matrices and its Applications*. Tokyo: Wiley.
- Tanaka, K. and Wang, H. O. (2004). *Fuzzy Control Systems Design and Analysis: a Linear Matrix Inequality Approach*. Hoboken, NJ: John Wiley & Sons.
- Wang, S., Pan, J., Nguyen, A.-T., Guerra, T.-M., and Lauber, J. (2021). “Takagi-sugeno fuzzy fault detector design with finite-frequency specifications for autonomous ground vehicles,” in *4th IFAC Conference on Embedded Systems, Computational Intelligence and Telematics in Control CESCIT 2021.IFAC-PapersOnLine*, 195–200. doi: 10.1016/j.ifacol.2021.10.033
- Wang, Z. Q., Viadero-Monasterio, F., Jimnez-Salas, M., and Lpez-Boada, M. (2022). Fault estimation for vehicle steering systems using a triple-integrator fault model and h/hinf observer. *IEEE Trans. Vehicular Technol.* 71, 5875–5888. doi: 10.1016/j.ress.2025.111573
- Zemouche, A., Boutayeb, M., and Bara, I. (2008). Observers for a class of Lipschitz systems with extension to H_∞ performance analysis. *Syst. Control Lett.* 57, 18–27. doi: 10.1016/j.sysconle.2007.06.012
- Zemzemi, A., Kamel, M., and Toumi, A. (2019). “Fault estimation based on t-s fuzzy intermediate observer for nonlinear system subject to mismatched faults,” in *2019 16th International Multi-Conference on Systems, Signals Devices (SSD)*, 294–299.
- Zhang, B., Du, H., Lam, J., Zhang, N., and Li, W. (2016). A novel observer design for simultaneous estimation of vehicle steering angle and sideslip angle. *IEEE Trans. Indus. Electron.* 63, 4357–4366. doi: 10.1109/TIE.2016.2544244
- Zhang, H. and Wang, J. (2017). Active steering actuator fault detection for an automatically-steered electric ground vehicle. *IEEE Trans. Vehicular Technol.* 66, 3685–3702.
- Zhang, L., Hu, M., Bian, Y., Zhang, H., and Nguyen, A.-T. (2025). Less-conservative robust path tracking control with intrinsic bump-free feature for autonomous vehicles: a sub-polytope integrated approach. *IEEE Trans. Intellig. Transport. Syst.* 26, 10428–10442. doi: 10.1109/TITS.2025.3554157
- Zhou, Z., Shojafar, M., Abawajy, J., Yin, H., and Lu, H. (2022). ECMS: an edge intelligent energy efficient model in mobile edge computing. *IEEE Trans. Green Commun. Network.* 6, 238–247. doi: 10.1109/TGCN.2021.3121961